Comparison between High-Velocity-Air-Fuel- (HVAF) and Cold-Gas-Spray (CGS) by evaluating mechanical properties of Ti-6-4- and INCONEL718-coatings

Nicolaie Markocsan*, Christophe Lyphout*, Lars G. Östergren**, Max Sieger***

* Production Technology Center PTC, Department of University West, Trollhättan/Uddevala, Sweden

** Volvo Aero Corporation, Trollhättan, Sweden

*** Technische Universität Dresden, Dresden, German

For contact:

nicolaie.markocsan@hv.se

lars.g.ostergren@volvo.com

max.sieger@gmx.de

abstract

Talking on thermal spraying a lot of different techniques like Plasma Spray, Powder Flame Spray, Wire Flame Spray as well as High-Velocity-Oxy-Fuel- (HVOF) and High-Velocity-Air-Fuel-(HVAF)spray [1] can be found to apply metals, oxides, ceramics, cermets, nitrides, carbides and also polymers [1] for wear and corrosion applications[1]. Every member of the thermal spray family propels more or less molten feedstock-particles towards a prepared surface where the so-called splats quench and rapidly solidify with a lamellar structure. The thermal energy is generated either by a chemical process or an electrical heating. Sprayed metals are usually harder than the accordant wrought metal due to the inclusion of dispersed oxides, but have limits in porosity, thickness and relatively low bond strength. Also the line-of-sight process is not able to coat every kind of shape.

The latest invention is the Cold-Gas-Spray-Process (CGS)[2] also called "kinetic energy metallization" or "high-velocity powder deposition", taking a unique role in thermal spraying by using low temperature and rapidly high velocities to form dense and adherent coatings by a high pressure compressed gas propelling the powder particles to supersonic speed through a convergent-divergent DeLaval-Noozle.

By operating in a solid state the CGS gives the opportunity of spraying titanium without the risk of oxidation by exceeding a critical temperature of 880°C and keeping a clean surface. Due to a lower specific weight compared to other metals like nickel, while giving good mechanical properties, the application of titanium is favored to save weight in aero planes.

Using a powder instead of rods and wires increases the degree of melting respectively decreases the necessary heat-input and produces thereby finer droplets and smoother coatings.

HVAF uses as mixture of combustible and air instead for pure oxygen (HVOF) for accelerating the powder stream trough the nozzle. This gives advantages in cost and the process is easier applicable. The flame temperature reaches 1000-1500°C depending on the combustible, achieving the same range of velocity like CGS. The process can be described as "warm kinetic spraying", positioned in between HVOF and Cold Gas-Dynamic Spraying.

The following paper presents the results of a prestudy on cold-sprayed and HVAF-sprayed coatings of Ti6-4 on Ti-6-4 and Inconel718 on Inconel, including microstructure analysis, surface roughness, Vickers- and Rockwellhardness, adhesionstesting by Glue- and Braze-Adhesion-Test and 4-Point-Bending, to find out if CGS is applicable for the repair of airplane assemblies in comparison to the established HVAF-Process.

Key-findings

Both materials and both techniques are able to reach high values in hardness, adhesion strength and favorable low values in the Young`s Modulus when being applied as a coating. A profound substrate preparation by grit-blasting and optimal spray parameters are needed to generate a low porosity and optimal anchorage of the splats to the surface, which seem to be a key to all mechanical values mentioned.

In comparison to HVAF-sprayed samples it could be revealed that CGS still needs to be improved by adjusting spraying parameters to get to the same level of performance. Still CGS seems a promising technique to spray oxidation-sensitive materials.

Introduction

First applied in the 1980s by A. Papyrin at the Institute of Theoretical and Applied Mechanics of the Russian Academy of Science in Novosibirsk, the solid-state deposition of metallic and non-metallic powders by cold spraying uses high-velocity particles (supersonic: Mach 2 till Mach 4, 300 up to 1200 m/s), propelled by a gas stream through a De Laval-nozzle, and process-temperatures between 0 and 700°C to form a dense and adherent coating on the substrate material via plastic deformation of the powder particles at the **high-kinetic impact** (fig. 1).

Using Nitrogen or Helium as process gases a low oxide content as well as a high deposition efficiency (20-80% [1, p.78]), high density, low residual stress, minimal heat input on the substrate (minimal grain growth) can be realized at powder feed rates up to 8 kg/h [1].

Influenced by interconnected parameters like standoff distance, powder feed velocity, particle velocity (above critical velocity to form a bond without particle-reflection, but below a value leading to solid particle erosion of the existing coat), particle and substrate temperature, nozzle geometry and the particle diameter (related to the critical velocity), the CGS is expected to fulfill the requirements for coatings with high wear-, heat-, corrosion-, oxidationresistance, specific electrical properties (semiconductors), gradient-materials, or metal composites without chemical reaction at low temperatures. Applications in aerospace, automotive, chemical industry as well as biomedical and electronic tasks can be handled by the unique microstructure of CGS-coats.

Being located in-between HVOF and CGS by its parameters particle velocity and temperature the HVAF-process is simpler in use because it uses cheap oxygen with unlimited supply from an air compressor. Compressed air enters the gun as a cooling medium before it is mixed with a gaseous fuel. The spray powder temperature can be controlled by the combustion parameters or by adding hydrogen to the process. A secondary combustion for fine-tuning is in use.

The Activated Combustion (AC)-HVAF [3] was patented by Dr. Baranovski in the 1990's. It opened a second era of HVAF-based equipment with higher Deposition Efficiencies.

Main advantages of the HVAF-process are being compatible with a wide range of fuels (propane, butane, propylene, ecofriendly natural or MAPP-gases), independency of a separate cooling unit, no nozzle-clogging, and inducing lower stress levels.

Ti-6Al-4V is a so-called Grade-5-(α+β)-Titanium alloy (tab. 1), first specified in 1954[4], with aluminum stabilizing the α-case and Vanadium stabilizing the β-case. Due to a high tensile strength and toughness even at extreme temperatures and an extraordinary corrosion resistance at a light weight compared to most other metals the material is used in airplanes and spacecraft applications as well as premium sports equipment. A low oxidationresistance, a low Young`s Modulus and high price for mining and processing even though high occurrence, are problematic when dealing with Titanium. A growing use in medical applications such as artificial bones due to the low Young`s modulus should be mentioned.

The nickel-based super alloy Inconel718 (tab. 1) is in widespread use in aerospace industry for its combination of high-temperature-stability, ductility, easy treatment and wear to corrosion and oxidation especially at high temperatures, reaching already 85% of the melting temperature in application[4].
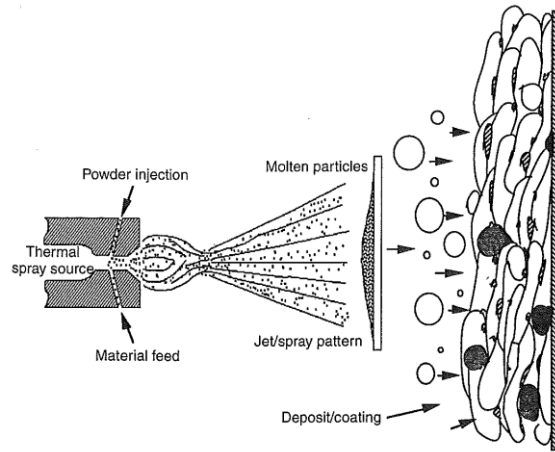
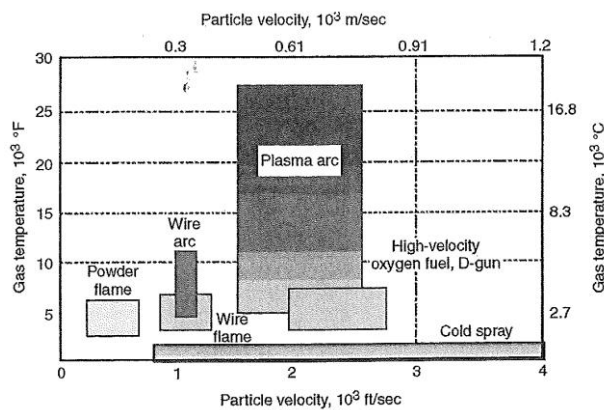**fig. 1:** schematic diagram of thermal spray processes[2]

Fig. 2: temperature/velocity regimes for common thermal spray processes compared to CGS [2]

tab.1: chemical composition (wt-%) Ti6-4, IN718[4][5][6]

Ti6-4	In718
Al: 6, Fe: <0,25, O: <0,2, Ti: 90, V: 4	Ni (+ Co [1% max]): 50,00-55,00, Cr: 17,00-21,00, Fe: Balance, Nb (+ Ta): 4,75-5,50, Mo: 2,80-3,30, Ti: 0,65-1,15, Al: 0,20-0,80, C: <0,08, Mn : <0,35, Si : <0,35, P: <0,015, S: <0,015, B: <0,006, Cu: <0,30

tab.2: specific values of Ti6-4 and IN718[4][5][6]

	Ti6-4	IN718
density [g/cm^3]	4,43	8,19 (annealed)
meltingpoint (solidus – liquidus)	1604 - 1660 °C	1260-1336 °C
ß-transus-temperature [^{o}C]	882	-
specific heat capacity [J/(kg $^.$K)]	526	435
CTE [µm/m$^.$K], linear (20 ^{o}C)	8,6	13,0
electrical resistivity [Ω/cm]	0,000178	0,000125
thermal conductivity [W/m$^.$K]	6,7	11,2
yield tensile strength $R_{p0,2}$ [MPa]	1030	1036
ultimate tensile strength [MPa]	1150	1240
elongation at break [%]	14	25
Young`s Modulus (20 ^{o}C) [GPa]	110	200

3

materials and experimental methods

The samples used in the experiments were sprayed at four different locations:

- Location B (CGS)
- Location A (CGS)
- Location C (SAF M3 gun)
- Location D (HVAF AK-07 gun)

The experiments on adhesion (glue and braze testing), hardness (Vickers and Rockwell), microstructure, residual stress (MLRM), surface roughness and 4-point-bending (extraction of Young's Modulus) were conducted at the Production Technology Center (PTC) as well as at the Volvo Aero Corporation (VAC) in Trollhättan.

substrate preparation:

- Location B: grit-blasting (Al$_2$O$_3$, Grit 24, 60 psi, 70°), aceton+air-cleaned
- Location C: grit-blasting (Al$_2$O$_3$, Grit 22)
- Location D -1,-2:grit-blasting at Location D
- Location D -3: grit-blasting at VAC

powder:

commercially available powders

tab.3: powders used

Location	Powder	Run	Size [µm]
B	AP&C Rayma Eli Powder Ti6-4	1	- 45 + 00
C	Dynamet Inco 718	1	???
	AMDRY 1781 IN718	2, 3	???
C	AP&C Rayma Eli Powder Ti6-4	1	- 45 + 00
A	MOGUL MTS 2433 HVOF Spray Powders "Type Inconel 718"	1	- 45 + 15
A	AP&C Rayma Eli Powder Ti6-4	1	- 45 + 00
D	???	1,2,3	???

samples:

tab.4: locations and samples - overview

Substrate Material	Location	process
TiAl6V4	Location B	CGS
IN718	Location C	SAF
TiAl6V4	Location C	SAF
IN718	Location A	CGS
TiAl6V4	Location A	CGS
IN718	Location D	HVAF

Three different sets of samples where used:

- coupons for adhesion, hardness, microstructure, residual stress measurement
- square plates for hardness, microstructure
- rectangular plates for 4-point-bending
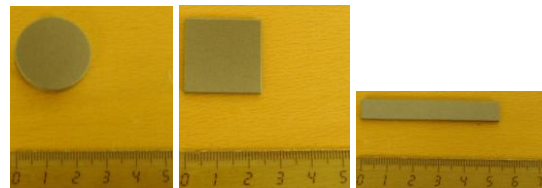
Fig. 3: coupon, square, rectangular

tab.5: sample specifications

Substrate Material		IN718		Ti6Al4V	
Geometry	Dimension (mm)	AMS	VAC	AMS	VAC
Coupons	Ø25.4 x 6.35	5662	141767	4928	141760
Sq. Plate	25.4x25.4x1.6	5596	156134	4911	156130
Rect. Plate	55 x 8 x 1.6	5596	1.60 mm	4911	1.83 mm

sample preparation:

cutting:

The coupons were cutted by using a Struers-machine with a diamond-cutting wheel with 2000 rpm under constant water-cooling. [7]

mounting:

Round samples of each location were cold/hot-mounted under vacuum by using a PTFE-mesh to avoid shrinkage-cracks.

Grinding and polishing:

The samples were prepared on a Struers Prepamatic machine by using a predefined program.

microstructure

According to ASTM E562-08 [8] a manual point-count on 30 evenly distributed fields with a 100-point-layer each on a Olympus BX60M with a JVC TK-C181 Color-video-camera, using the Piscara 9.4-software was conducted, from which the porosity could be calculated.

adhesion (glue and braze testing)

According to ASTM C633 [9] a tensile-strength-test on glued and brazed coatings with a surface-diameter between 23 and 25mm of the suitable bond agent FM1000 (Polytetrafluorethylene, Cytec Fiberite, Winona, MN) between coated sample and a counter-metal-coupon respectively a brazing, was conducted on a ZWICK Z100-tensile-test-machine at a tensile-speed of 0,1 mm/min. All tests were performed at room temperature until rupture occurred

hardness

Rockwell

To get an insight on the approximate hardness of the coating materials one sample of Ti6-4 and IN718 each were measured in an as-sprayed state. From those values a minimal coating thickness after grinding was calculated.

After preparation by grinding of 50µm of the coating in two steps (grind-papers 120 and 320, without water; 300rpm), and grinding the bottom side to a parallel surface (papers 120, 500, 1000; 300 rpm) with a Struers Planopol machine, the samples were cleaned in Ethanol and Acetone and dried with hot air. [10]

The Rockwell Superficial Hardness HR15N was measured with a INDENTEC 8150K with 15 kgf (147N) force with a diamond-indenter.

According to VAC-standard procedure [11] (dependent on ASTM E18-08b [12]) twenty indents in evenly spaced positions over the whole surface were placed.

Vickers

Vickershardness HV0,3 (300g force) was measured on a Micromet 2101 (Buehler)-machine (Omnimet MHT software-package, magnification x400) according to VAC-standard procedure [13] (dependent on ASTM E-384 [14]) by twenty indents each on cold/hot-mounted, grinded and polished samples.

surface roughness

The surface roughness was tested with a Mitutoyo SJ301 equipped with a 5µm radius diamond tip (ISO 1997 GAUSS, λc 0.8mm X5 Range (Auto)). It was calibrated using a calibration surface (Ra ~ 3 µm) and drawn at 0,05 mm/s. All samples were air-sprayed for cleaning; different directions of testing were used, as well as different areas.

10 tests were conducted on each sample, the roughness values R_a and R_z have been evaluated. [15]

<u>4-point-bending test:</u>

Three rectangular samples of each examined coating were bend in a ZWICK Z100-machine at room temperature using a 4-point-bending-fixture and the testXport Radek Series 5 – software until rupture or reaching the machine-limits.
The tests were conducted in tension-mode at 10N pre-force with a bending-velocity of 0,1mm/min, no significant difference between tension and compression-mode could be examined in preliminary tests.

Stresses induced by cutting and grit-blasting were analyzed in a separate test series on Almen Strips [5][6], bending them in the linear area of the stress-strain-curve.

The Young`s Moduli of the substrate materials were examined on rectangular samples of the same dimensions and conditions.

The Young`s Moduli of the coatings were calculated by using formula (1) [16]

$$\frac{b\left(d_h^4 E_h^2 + 2 d_h d_s \left(2 d_h^2 + 3 d_h d_s + 2 d_s^2\right) E_h E_s + d_s^4 E_s^2\right)}{12\left(d_h E_h + d_s E_s\right)} - F \cdot a \cdot \frac{g^2}{2 \cdot f^*} = 0 \tag{1}$$

$$EI = F \cdot g^3 / (2 \cdot f^*) \tag{2}$$

$$I = d^3 \cdot b / 12 \tag{3}$$

$$\rightarrow \quad E = 6 \cdot F \cdot g^3 / (d^3 \cdot b \cdot f^*) \tag{4}$$

h: coating   s: substrate
b: sample-width   d: sample-thickness
E: Young`s Modulus   I: bending stiffness
F: force(**OBS**! Force applied on one
        holder! = ½ full force)
a = g = l = 10 mm
g: distance between outer clips
f*: deflection measured using a 3-point
    clip-on-device

Results and Discussion

<u>Microstructure:</u>

Porosity
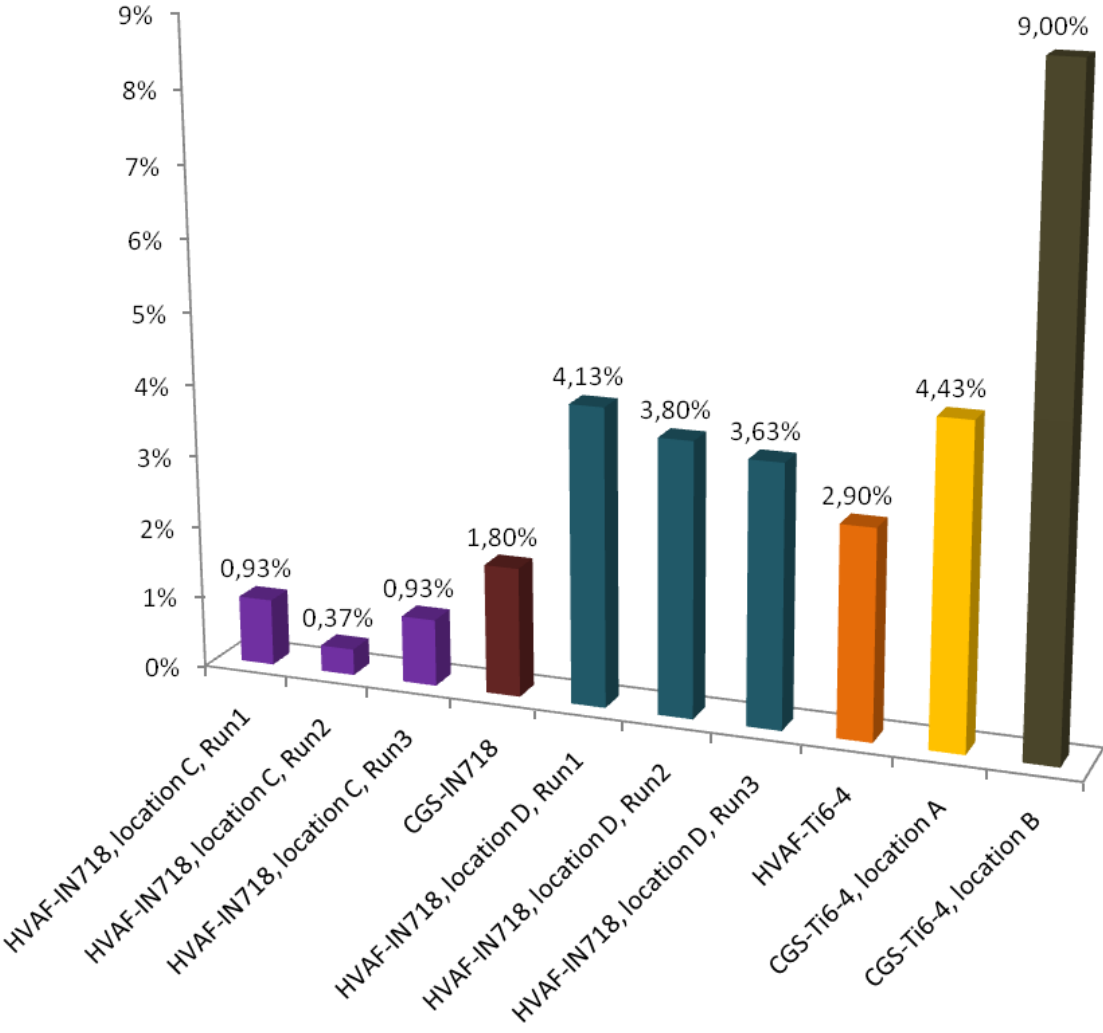
Fig. 4: porosity by manual point-count

Point count analysis on the prepared sample-cross-sections gave an insight on porosity, grit-residues, oxides and particle-deformation.

Inconel718 showed higher densities than Ti6-4, as well as the HVAF-process could accomplish higher values compared to CGS.
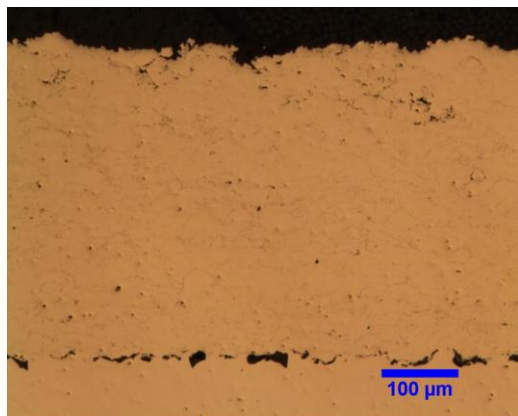
Using the same metal-alloy-powders for spraying at all locations, the different results are related to the processes themselves (temperature, velocity) as well as the spraying parameters used at the different facilities.

Using higher temperatures the HVAF-process is providing a fillup of voids by higher plastical deformation of the single powderparticles (droplet-forming). Therefore the HVAF-samples sprayed at higher velocities showed the highest densities but also had the highest amount of grit-residues apparently belonging to a excessive extanded Al_2O_3-grit-blasting-process-time.
HVAF-samples which were sprayed with a lower particlevelocity showed a higher porosity as well as more big cracks could be found in them (see fig. 7). A lower particle velocity and therefore a slower coatingformation leads to cracks during particleshrinkage.

Also a comparison fig. 7 and 8 points out the differences in surfacepreparation. The advanced surfacepreparation by Grit-Blasting enables a better mechanical interlocking at the interface, also leaving less residues.

HVAF-sprayed Titanium (fig. 11) showed clearly higher oxid-content related to the high process temperature exceeding the critical temperature of 880°C when a chemical reaction Ti + O_2 → TiO_2 starts. Also the porosity-content was quite high, as well as a lot of half-molten particles could be found.

Highest porosity could be found on CGS-Ti6-4 from location B, which had problems while spraying. Clogging issues at the noozle and a malfunction of the rotational speed are clearly the reasons for the observed microstructure.

For industrial applications a lot of factors have to be considered: Porosity is detrimental with respect to corrosion, macrohardness, strength, wear characteristics, but also can be important with resect to lubrication, shock resisting properties, reducing stress levels, increasing thickness limitations and adrability in clearance control coatings.

Fig. 5: HVAF-sprayed IN718 Location C (higher velocity) (x100)
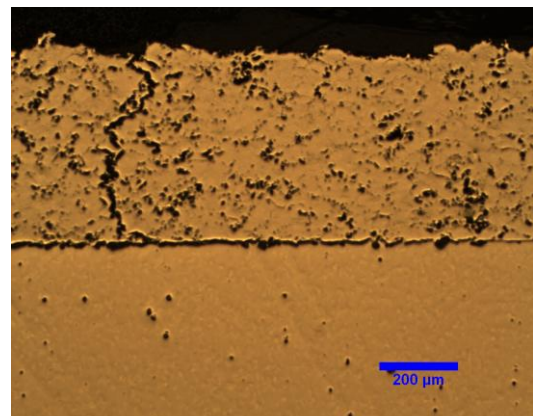
Fig. 7: HVAF-sprayed IN718 Location D (lower velocity) (x50)
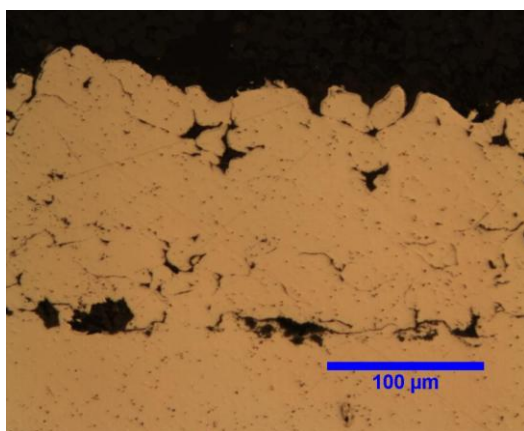
Fig. 6: CGS-sprayed IN718 Location A (x200)
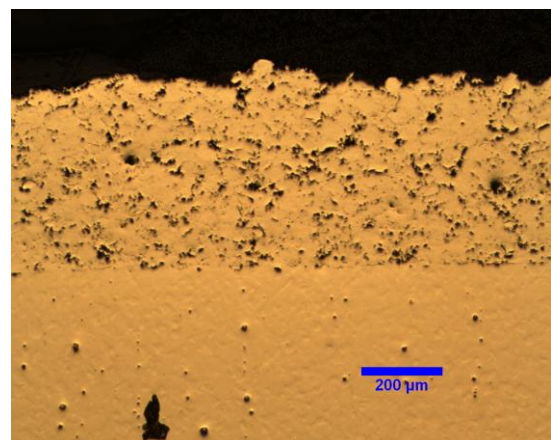
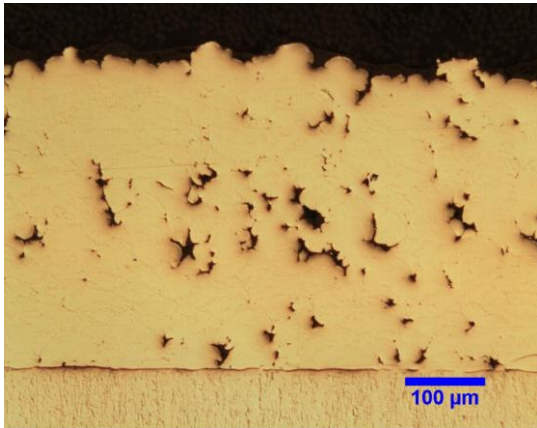**Fig. 8:** HVAF-sprayed IN718 Location D-3 (lower velocity, advanced Grit-blasting) (x50)

8

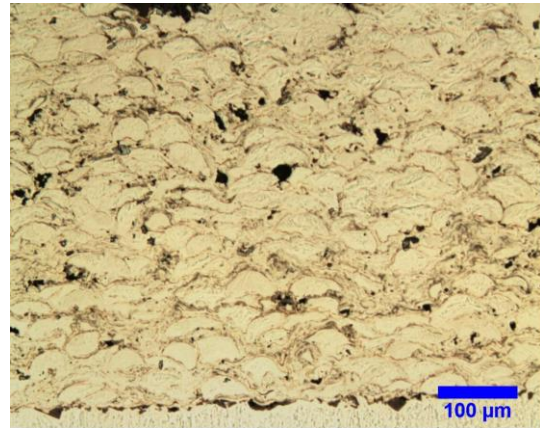**Fig. 9:** CGS-sprayed Ti6-4, location A (x100)
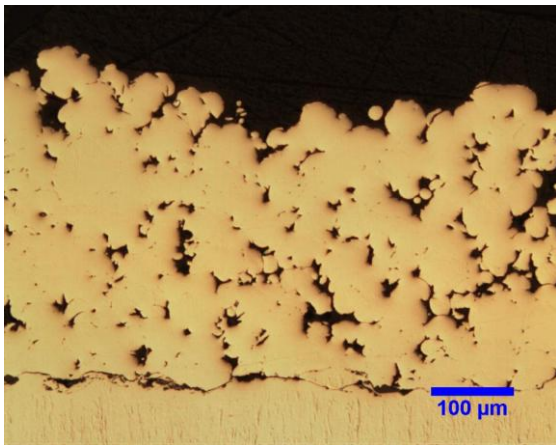

Fig. 11: HVAF-sprayed Ti6-4 Location C (x100)

Fig. 10: CGS-sprayed Ti6-4, location B (x100)

tab.6: coating thicknesses

	coating thickness [µm]
CGS-IN718	150
HVAF-IN718, location C, Run1,2	450
HVAF-IN718, location C, Run3	1000
HVAF-IN718, location D, Run1	600
HVAF-IN718, location D, Run2	500
HVAF-IN718, location D, Run3	450
CGS-Ti6-4, location A	390
CGS-Ti6-4, location B	350
HVAF-Ti6-4	500
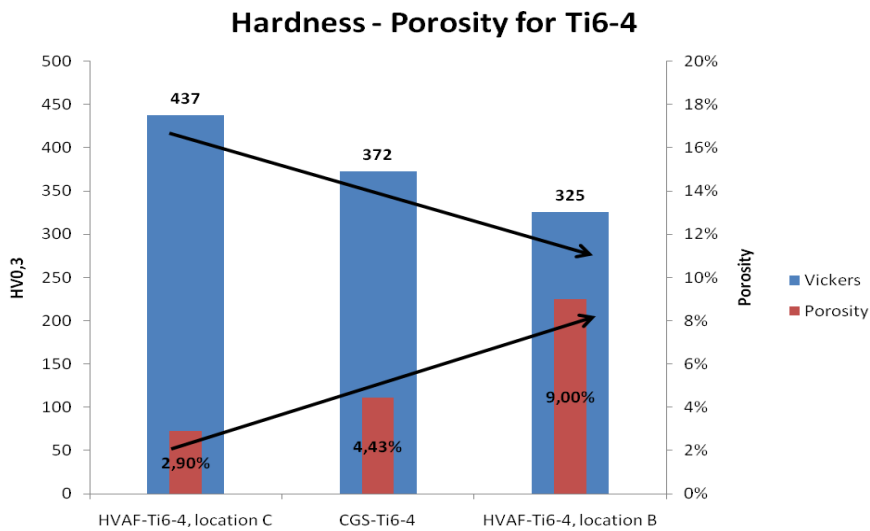
Fig. 12: comparison hardness/porosity for Ti6-4

Fig. 12 shows the clear relationship between porosity and hardness. The effect

Porosity ↑ = Hardness ↓

is pointed out just for Ti6-4 with the higher differences in porosity between the different sets, but was found for IN718 as well.

9

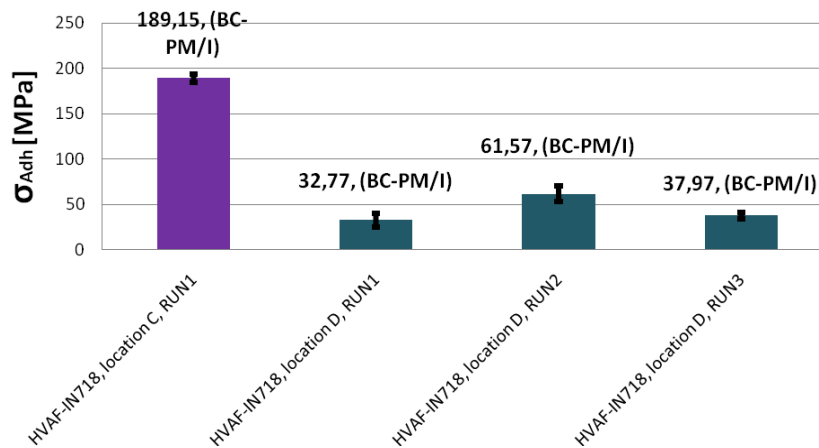adhesion testing (by glue and braze testing)

HVAF excels CGS again as Inconel718 shows higher adhesion values than Ti6-4.
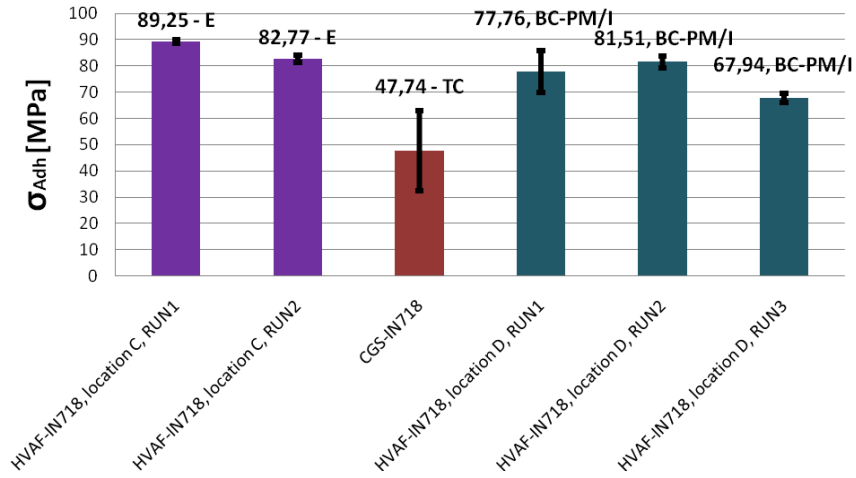
Fig. 13: adhesionstrength IN718-sets by glue-test
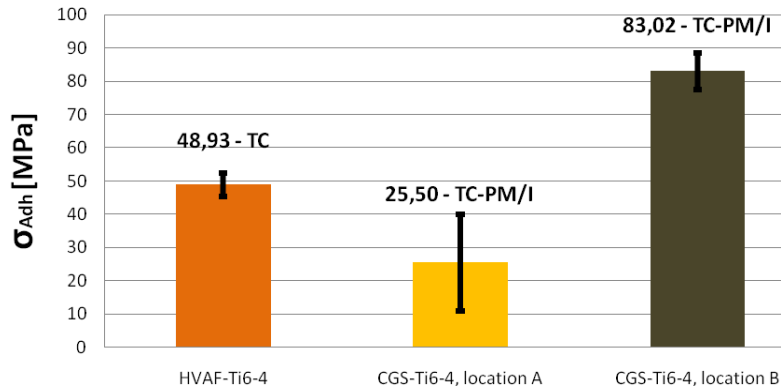
Fig. 14: adhesionstrength Ti6-4-sets by glue-test

Fig. 15: adhesionstrength In718-sets by brazing-test

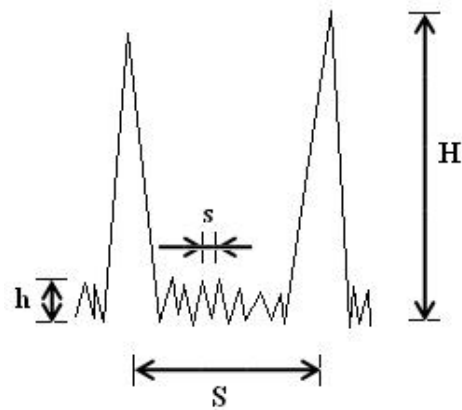E – Epoxy; TC – Topcoat; I – Interface; PM – Parent Metal

Fig. 16: failure at the substrate-coating-interface (I)

Fig. 18: coating-failure (TC/PM-I)

Fig. 17: glue-failure (E)

Fig. 19: draft of a surface with two distribution by 2-step-grit-blasting; S,s: spacing; H,h: height

(mechanical interlocking around the hills and in the valleys is given at best for this roughness-distribution)

In accordance with the lowest porosity and a high interlocking the HVAF-Inconel718 shows the highest adhesion, even higher than the value of the used gluing agent (glue-failure),what makes a brazing-test (>80 MPa) acquired to find out the real value of 189,15 MPa.

Different failure-modes occurred:

Having a high adhesion strength HVAF-IN718 sprayed with higher velocities exceeded the glue and broke inside the gluing-region.

HVAF-IN718 sprayed with lower velocities broke all in the interface-region caused by inappropriate surface-preparation (see

interface region fig. 7) respectively a crack (also fig. 7) through the coating propagating along the interface. The spraying conditions leading to those cracks were already discussed above.

Although being very porous CGS-Ti6-4 from location B (fig. 10) also broke in the interface region at values that could have exceeded the glue as well. A penetration of the high porous coating (9,00%) is possible in this case.

HVAF-sprayed Ti6-4 showed a lot of oxides (fig. 11). Oxidation during spraying is the cause for failure in the coating (fig. 18). Cracks are propagating along the imbedded hard oxides.

11

Not being grit-blasted before the CGS-Ti6-4 from location A showed a clear failure at the substrate-coating-interface. The lack of required surface roughness and therefore mechanical anchorage between substrate and coat leads to a predictable interface-failure (fig. 16) and the low adhesionstrength.

As can be seen a high quality of surface preparation is of high influence for the adhesion strength.

According to Babhou et al. [17] a surface-preparation by grit-blasting is still state-of-the-art excelling other methods like hydrodynamic profiling, ice-blasting, electric discharge texturing, acid pickling and laser ablation. A maximum of adhesion strength is given at a spraying angle of close to 90°, grit-residues have their maximum at 75°.

A 2-step-grit-blasting (first step blasting with coarse grain, second step blasting with fine grain) could enhance the adhesion strength of thermal sprayed coatings by giving a surface texture with two distributions (see fig. 19) with a fairly good adhesion strength and fairly low grit-residue-content.

J. Wigren [18] evaluates the surface roughness to be at a maximum just before the content of grit-residues starts to rise immoderate, what leads to an optimal blasting time. Also a surface-cleaning with chemical methods is for some materials suitable.

Grit-residue-contaminations affect the adhesion as well as the low-cycle-fatigue (LCF)-properties (→ crack-initiation and -growth at residues), the diffusion between coating and substrate (→ chemical interlock), the wetting properties of impacting powder-droplets (→ Young`s law) and the residual stresses (→mismatch of CTE [coefficient of thermal expansion]) in a negative way, what gives the necessity of as little grit-residues as possible.

The differences between glue-adhesion-strength and the level of adhesion-strength evaluated by the brazing-test might result from the heat-input during the brazing, relieving the stresses which were introduced by peening and shrinking in the coating and interface-region. Further investigation of the residual stress-level by the MLRM is required here. A low stress level leading to high adhesion-strength for the HVAF-IN718-samples from location C (Fig. 15, violet) is expected. The lower braze-adhesion compared to the glue-test for the HVAF-sprayed IN718-setsfrom location D might be linked to a spallation of the coating from the substrate under heatinfluence when expanding. Also the coating-thickness might play an important role here.

This shows the effect of a possible post-heat-treatment that can affect the stress levels are thereby the adhesion strength.
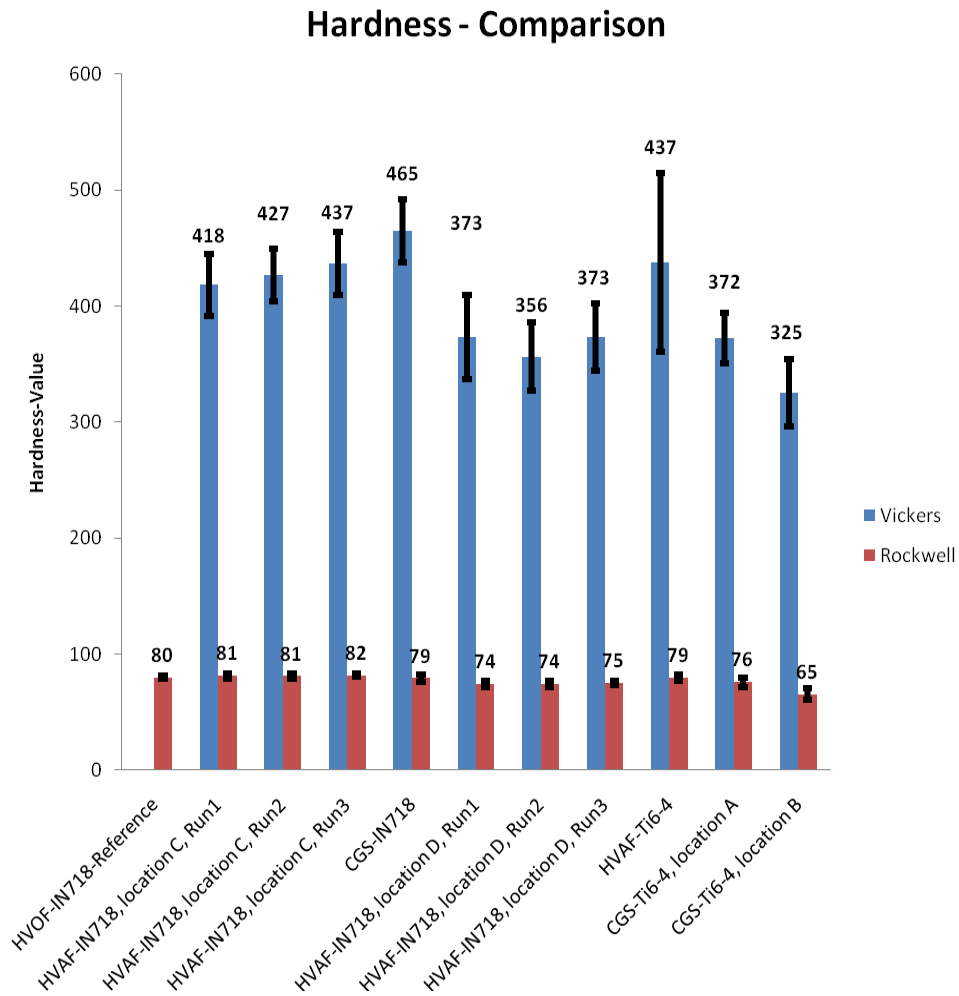
hardness

Hardness - Comparison

Fig. 20: Rockwell- and Vickershardnes

tab.7: hardnessvalues

	Vickers HV0,3		Rockwell HR15N	
	Ø	σχ	Ø	σχ
HVOF-IN718-Reference			**79,9**	1,3
CGS-IN718	465	27	**79,2**	3,2
HVAF-IN718, location C, Run1	418	27	**81,2**	2,4
HVAF-IN718, location C, Run2	427	23	**81,1**	2,5
HVAF-IN718, location C, Run3	437	27	**81,7**	1,5
HVAF-IN718, location D, Run1	373	36	**74,3**	2,8
HVAF-IN718, location D, Run2	356	29	**74,3**	2,8
HVAF-IN718, location D, Run3	373	29	**75,3**	1,9
CGS-Ti6-4, location A	372	22	**75,8**	4,2
CGS-Ti6-4, location B	325	29	**65,2**	4,9
HVAF-Ti6-4	437	77	**79,5**	2,5

13

According to the porosity-values of the manual point count Ti6-4 shows a slightly lower hardness than the highest values achieved by IN718 (Fig. 20) for Vickers- as well as for Rockwellhardness .

As hardness is defined as the resistance against the intrusion of another body into a material, high porosity leads to a low hardnessvalue, as also shown in Fig. 11.

Dense coatings show a hardness comparable or higher than the bulk-hardness due to work-hardening effects and peening-stresses by the powder particles impinging the substrate and lower coating-areas.

The higher hardness of oxides compared to the bulkmaterial should be considered, but is exceeded by the effect of porosity.

A statistical-t-test (statistical test based on the student-distribution of William Gosset) was used to determine whether the differences between the hardnessvalues could be considered statistically significant or not. The t-test gives the probability that the difference between two mean-values is caused by chance.

The t-test is defined as:

$$t = \frac{signal}{noise} = \frac{\text{difference between group means}}{\text{variability of groups}}$$

No significant statistical differences could be found between the hardness-values of squares and coupons as well as between the different Runs of each set.

R_a- In718
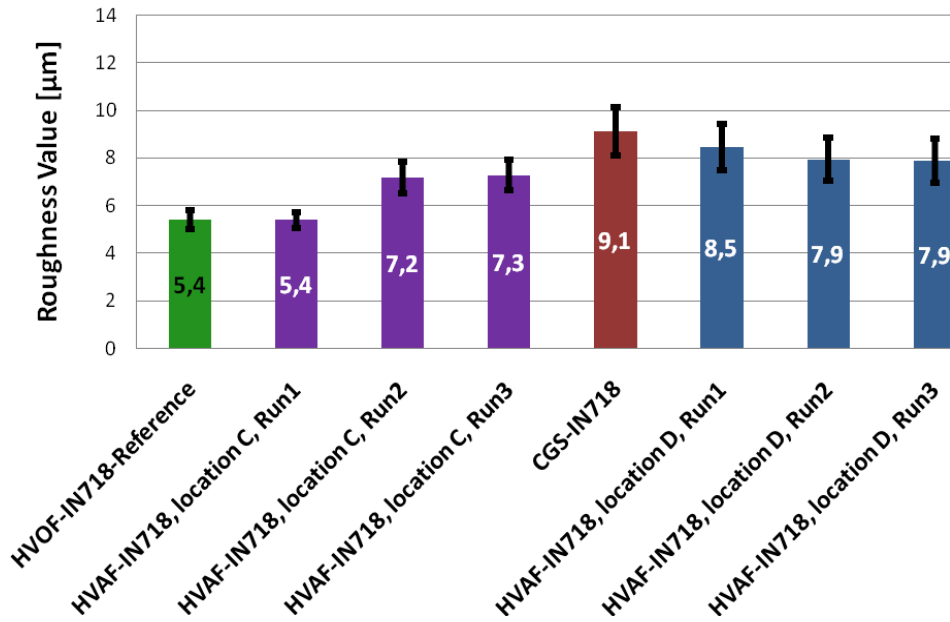
R_z- In718
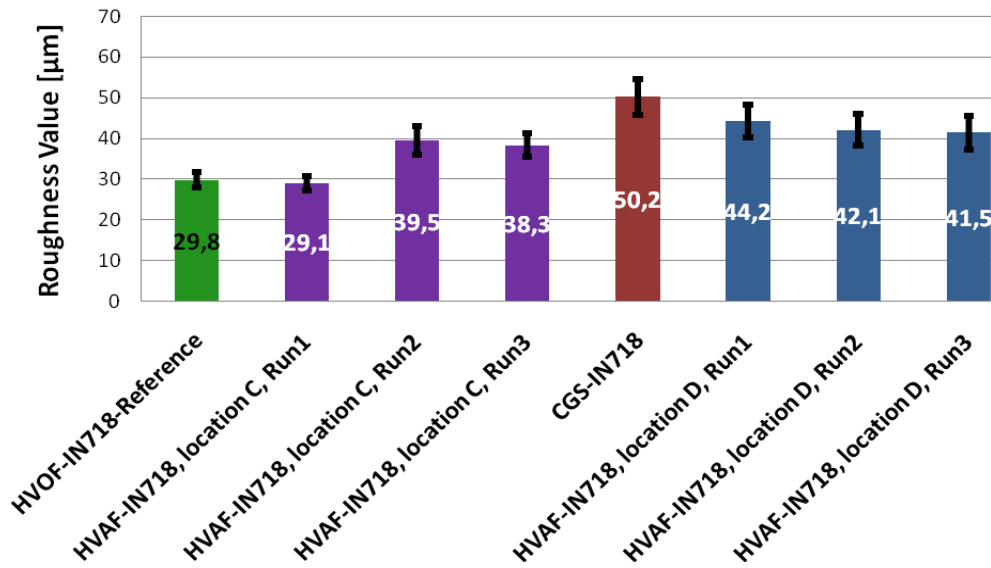
Fig. 21a: surface roughness - R_a
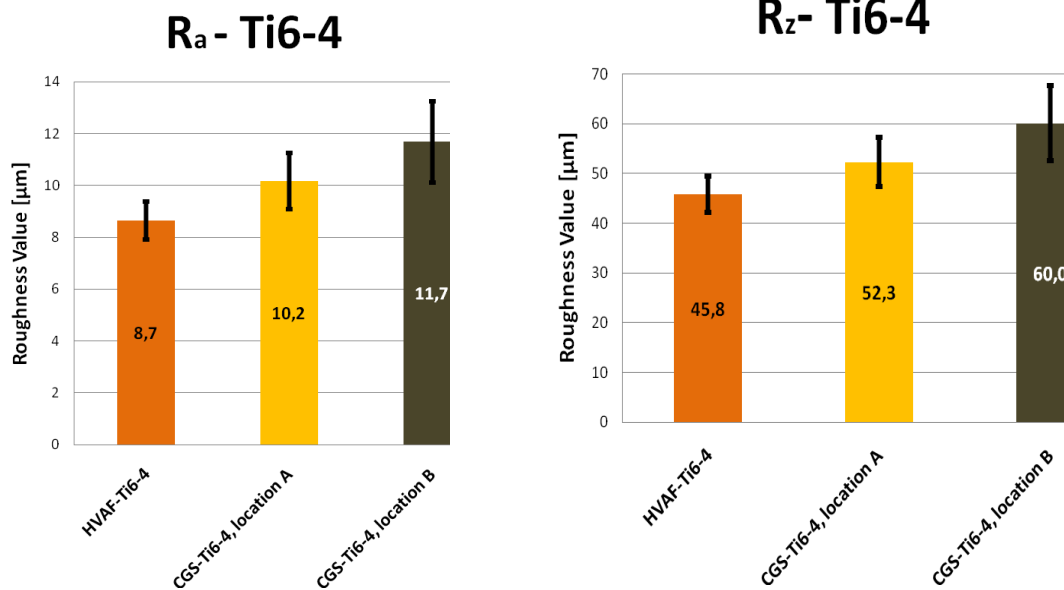
Fig. 21b: surface roughness R_z

Surface roughness evaluation by mean roughness value R_a and arithmetic average of peak to valley R_z showed lower values for the Inconel718 compared to the Ti6-4. R_a and R_z showing the same trend for both materials when comparing the different locations like expected.

Higher process temperatures in HVOF and HVAF generate a smoother surface than the CGS-process by partial melting the powder particles and making it easier to deform and flatten at the impact on the surface.

The highest roughness values are achieved by CGS-Ti6-4 from location B are clearly related to problems while spraying again.

Surface roughness needs to be considered for wear resistance and fluid flow processes along the surface. A favorable roughness of 6…10µm for further coating-applications like polymers for corrosion-resistance is achieved by all samples except on set, but can also be produced by surface-preparation like polishing afterwards. A low R_a can be increased by surface-preparation of the coating if necessary (→ mechanical interlocking of next layer).

It should be pointed out that by measuring R_a and R_z just amplitudes of the roughness can be evaluated. A spacing parameter between valleys/hills like R_{sm} (DIN EN ISO 4287)

$$R_{sm} = \frac{1}{n} \sum S_i \quad \text{(mean spacing)}$$

would also be suitable. Further details can be gained by fractal analysis [17].

J Wigren [18] mentions an maximal surface roughness which is achieved after an optimal surface-preparation (blasting)-time, breaking most of the oxide layers and just before overblasting the surface by flattening the peaks by further impacts again.

16

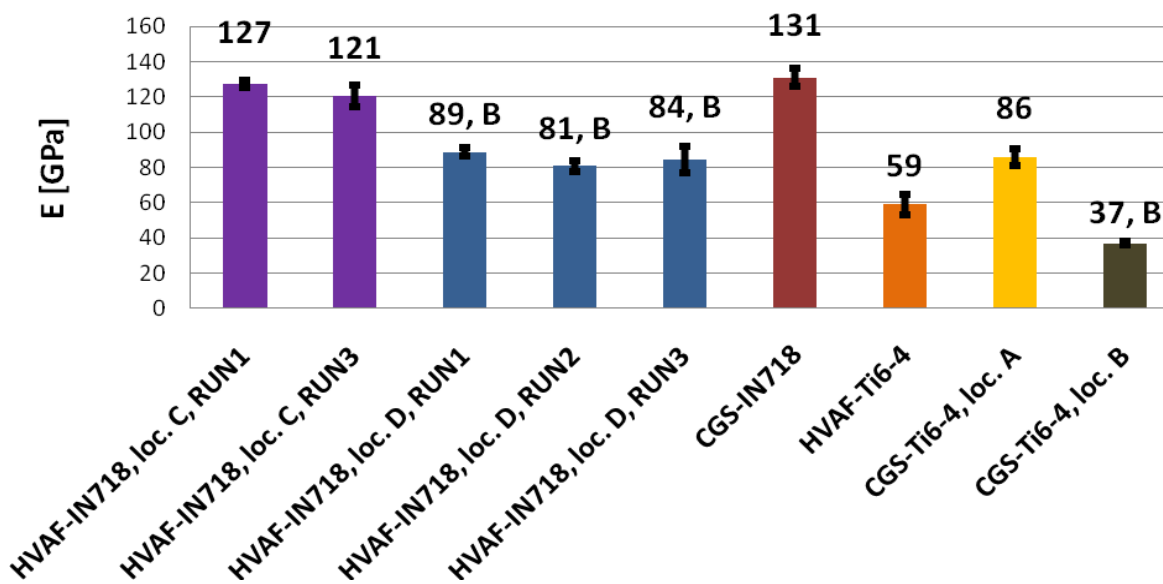<u>4-point-bending</u> <mark>OBS! ONGOING RESEARCH</mark> **(ABB-samples)**

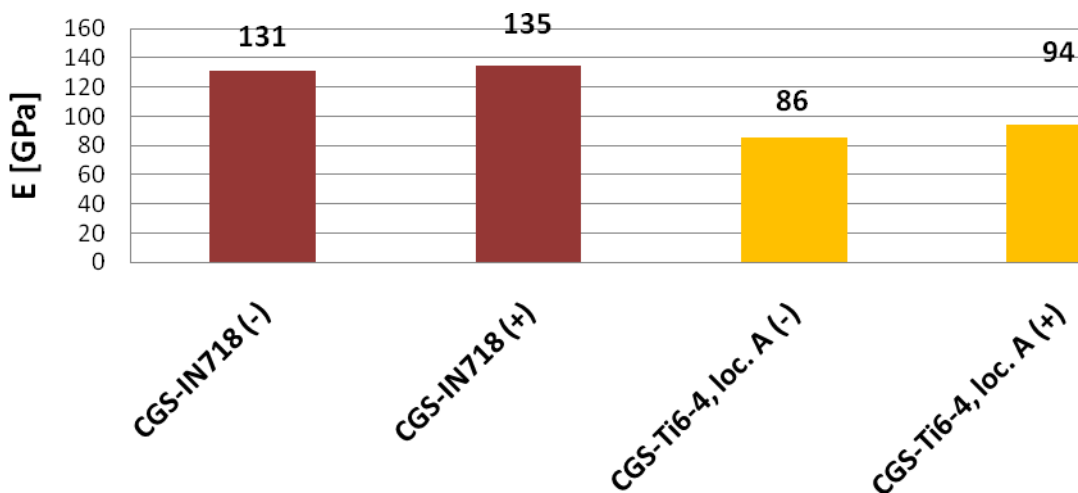**fig. 22:** Young`s Modulus evaluated by 4-point-bending (all tension, B: coating broke)

**Fig. 23:** Young`s Modulus: comparison between tension and compression (+)

Tab.8: maximum applicable force

	maximum applicable force [N]	
	tension (-)	compression (+)
CGS-IN718	580	730
HVAF-IN718, location D	620	850 (maximum machine force)
CGS-Ti6-4, location A	850 (maximum machine force)	850 (maximum machine force)

According to formula (1) the Young`s Modulus of the coating was calculated using the slope of the 4-point-bending-curve, the coating- and sample-thickness as well as the Young`s Modulus of substrate, evaluated in a separate experiment.

The Young`s Moduli of the substrates (calculated by formula (4)) were evaluated to be exactly even to the literature values of 110 GPa (111±2GPa) for Ti6-4 and 200 GPa (201±11 GPa) for IN718.

17

A low Young`s Modulus gives a ductile behavior which makes a material easier deformable. Cracks will therefore propagate slower; the energy needed to propagate the crack is higher; areas near to the crack have to be plastically deformed, making the crack itself stable until this energy-level is reached and stopping further growing. One could also say the fracture toughness is rising by a decreasing Young`s Modulus (see fig. 24).
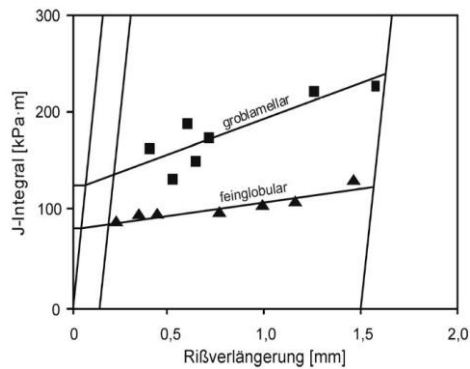
Fig. 24: fracture toughness of Ti-6-4, J-Integral by crackpropagation for a coarse-lamellar and a fine-globular sample [4]

Ti6-4 proved to have a much wider elastic range, not being plastically deformed by the maximal force applicable force of the ZWICK-bending machine (see fig. 25). IN718 showed just a small elastic area before changing its slope in the deflection-force-diagram by getting plastically deformed (fig. 26)

CGS- as well as HVAF-applied IN718-coatings could achieve about 65% (130 GPa) of the substrates Modulus, showing no effect of the coating thickness on the Modulus (double coating thickness for HVAF-sprayed IN718, location C, Run3).

The HVAF-sprayed IN718-samples from location D which showed big cracks broke at about 620 N applied force, showing also a lower Young`s Modulus as expected by taking into consideration the lower particle velocity forming a weaker bond.

The amount of pores inside the CGS-Ti6-4 from location B is also the cause for the break inside the coating here, still reaching higher values of maximum applicable force (≈750N).

The CGS-Ti6-4 from location A showed values reaching nearly a Young`s Modulus comparable to the value of the substrate (80%). A highly dense and well-bonded (fig. 9) microstructure gives best performance here. Still the low coating thickness (tab. 6, 150µm) leads to a comparable low maximum applicable force (≈580N in tension).

HVAF-Ti6-4 contrariwise shows a lot of half-molten particles as well as a globular microstructure (fig. 11) making it easier deformable and thereby softer.

fig. 25: strain(travel distance)-force-diagram for a 4-point-bended Ti6-4-substrate-rectangular
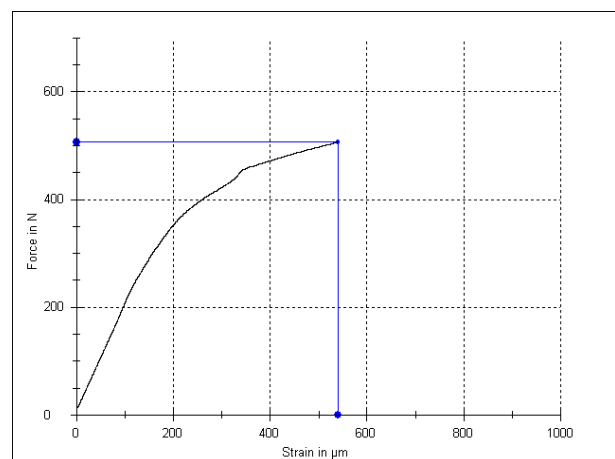
fig. 26: strain(travel distance)-force-diagram for a 4-point-bended IN718-substrate-rectangular

A lower Young`s Modulus compared to the bulk material was predictable, because the Young`s Modulus is a value for deformability of a material according to

$$\sigma = E * \varepsilon \ (Hooke`s\ Law).$$

Plastically deformation is much easier in a more globular microstructure applied by both spraying processes than in the bulk-material with lamellar grains. Therefore the bulk is stiffer than the coating.

Another factor affecting the stiffness is the grain-size. A lower grain-size can be applied by the low-temperature CGS which is not propagating grain-growth in a way like a high-temperature process does. Low grain-size leads to easier deformation because the grain can glide easier (see Ti6-4 in fig. 22).

It is clear that cracks will be propagated in the coating much easier when tearing their edges apart respectively a closing of cracks and voids will happen when applying a force to push their edges together. When this closing-process stops, material is pushed together and the material seems stiffer (slightly higher Young`s Modulus in compression, fig. 23), vice versa when tearing apart the coatings elastic and plastic deformation makes the material softer until the coating fails[19].

Also the maximum applicable force (see. Tab. 8) for IN718 is higher in compression mode compared to tension for the same reasons.

Evaluating the level of stresses being induced by grit-blasting the Almen Strips, it could be evaluated that grit-blasting had slightly no effect in IN718 but is hardening Ti6-4. (see Tab. 9, calculation by formula (4))

tab.9: 4-point-bending on Almen Strips

Material	grit-blasted		ungritblasted	
	Ø	σ	Ø	σ
IN718	176	15	188	13
Ti6-4	112	2	88	4

A work-hardening-effect by inducing peening-stresses can be pointed out here.

Being stiffer by its microstructural composition (lower porosity, higher density) IN718 is less deformable, so stiffer, and also more fragile to cracks but also harder.

On Ti6-4 impinging particles can induce vacancies which interact with other vacancies by repulsion. Taking into focus that deformation is caused by the movement of vacancies, the more vacancies repulsing each other the harder it gets to deform a material.

Testing the same stripes again in compression after bending them in tension related to the grit-blasted side, lower values of the Young`s Modulus were evaluated for IN718. The drop by around 20GPa can be explained by cracks and plastic deformation induced during the first bending. No effect of bending the rectangular again in the other direction could be evaluated for Ti6-4-Almen Strips. As described before the lower stiffness and wider elastic range of Ti6-4 is less fragile to crack induction and propagation.

Conclusion

tab. 10: Overview about the evaluated mechanical properties

+ higher value - lower value	Process				Material	
	In718		Ti6-4			
	HVAF	CGS	HVAF	CGS	IN718	Ti6-4
Adhesion	+	-	+	-	+	-
Surface Roughness	-	+	-	+	-	+
Hardness (HR15N, HV0,3)	≈		≈		≈	
Porosity	-	+	-	+	-	+
Young`s Modulus	≈		-	+	++	+

<u>**Materials:**</u>

Inconel718

Inconel718 showed better mechanical properties in all evaluated fields like expected from the higher values of the substratematerial (tab. 1) compared to Ti6-4 in all evaluted fields.

Giving highest advantage to the use in aerospace is the clearly higher adhesionstrength, exceding even the test-boundaries.

A lower Young`s Modulus of Inconel718-coatings compared to bulk-material shows a ductile behaviour, which can handle cracks better than a stiff sample.

Comparing the different spraylocations location C showed a lower porosity, but without further knowledge of all spray parameters (angle, spray-off-distance, mass-flow of gas, gas-pressure, nozzle shape, spray distance, particle size, powder preparation, substrate temperature, rotation speed of workpiece, powder-feed-rate, …) no conclusions can be drawn.

Also thermal and magnetical (tab. 1) properties should be considered, which were not evaluated in this study at all. Thermal properties are strongly related to the appearance of residual stresses. Inconel 718 losses its ferromagnetic properties at a curie-temperature of $-112^{o}C$ and is just paramagnetic at normal and elevated temperatures.

Still the higher weight of the nickel-based superalloy needs to considered when talking on the economic aspect of aeroplane-applications. (*weight = money*)

Ti6-4

Having lower values in all evaluated properties Ti6-4 nevertheless should not be seen as a weaker material for the favored applications, but more as a metal unadjusted to the processes with huge possibilities.

HVAF-Ti6-4 shows a very ununiform microstructure (see fig. 11) with lots of oxides and halfmolten particles due to the high process temperature. Still the mechanical values are quite high and reach the level of the other samples, except for a very high standard deviation in all results. Further investigations should be done here.

Having not as high values as Inconel718, Ti6-4 still achieves still high levels of hardness (tab. 7), quite good porosity-values (fig. 4) and a more ductile (lower) Young`s Modulus (fig. 22) as CGS-coat in comparison to a Ti6-4-bulk, favouralbe for better crack-growth-properties.

The most important problem to solve for the applicability in aerospace is to boost the adhesive strength between titanium-coatings and substrate-materials and strengthening the mechanil interfacebond. Otherwise Ti6-4 seems not be able to get on eye height with Inconel 718, although having the huge opportunity of being a leightweight.

It is clear that all mechanical values are related to the microstructure of a material and its phases.

Ti6-4 normally has a lamellar microstructure (see fig. 27) when cooled down from the β-phase (β-transus-temperature = 882 ^{o}C), but can be made globular by heat-treatment (recrystallization) as

well as being applied globular or in between globular and lamellar (droplet flattening at the impact) by thermal spraying.
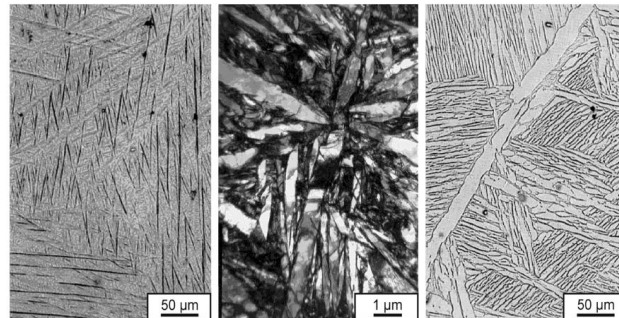
Fig. 27: fine-, coarse-lamellar, and martensitic Ti6-4 (optical microscope, TEM) [4]

A globular microstructure gives better properties when dealing with cracks, like discussed in the 4-point-bending-section. The grain-size is an important factor here as mentioned before.

A fine grain gives advantage to strength as well as ductility (→ used in grain-size-hardening: Hall-Petch-Equation $\sigma_y = \sigma_0 + k_y/d^{½}$ [20]) and also to resistance against oxidation and crack induction, but a coarse grain shows less crack propagation and higher creep rupture strength.

A finer microstructure can be applied by CGS due to lower process temperatures.

A lamellar microstructure advantages fracture toughness, crack propagation and oxidationresistance, but corrupts strength, ductility and crack induction. A lamellar microstructure has a higher creep resistance for this reason (see fig. 28)
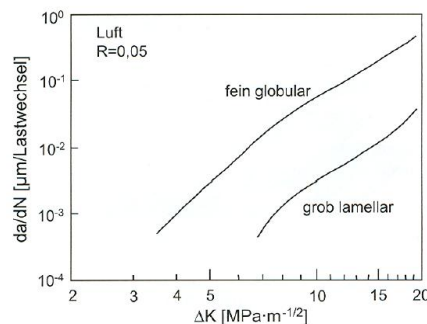
Fig. 28: alternation of load about fracture toughness for a fine-globular and the coarse-lamellar Ti6-4 [21]

At elevated temperatures the chemical reaction Ti + O2 → TiO2 takes places leaving a hard and brittle oxygen layer called α-case. To get along with this problem Chen et. Al[21] invented a method to deoxygenate the alpha case on CP titanium and the Ti-6Al-4V alloy by cathodic refining in molten $CaCl_2$. They could reach a satisfactory level within 1 hour at 950°C without altering the microstructure, composition, and dimension of the material.

Processes:

Dividing up the results by the different processes used, it can be seen the HVAF-process gives less surface roughness (fig. 21), slightly higher hardness-values (tab. 7) and less porous coatings but here with dependency on the spray parameters. Depending on mechanical interlocking and the surface preparation as discussed above, the adhesion (fig. 14) strength has also higher values.

Being the process with much higher temperatures compared to CGS single-droplets can deform much easier when impacting on the surface, leading to more flattened and therefore more even surfaces. Filling up voids and closing pores by penetrating them in molten or half-molten better deformable state, HVAF-droplets form a denser coating leading to higher values in hardness (compare for example IN718: fig. 5 [HVAF, dense] and fig. 6 [CGS, porous]) and adhesion (fig. 14).

The process temperatures of HVAF (1000-1700°C [2]) exceed the temperature at which Titanium starts to oxidize and therefore a lot of half molten particles and oxides can be found in Ti6-4-UnC (fig. 7). Still a hard, adherent, fairly dense coating remains in this case.

The CGS-process proved himself as a useful tool for oxidation-sensitive materials as Titanium and materials with a low melting point like polymers, also implying lower levels of residual stresses due to a lower shrinkage-rate. Neither spraying-residues nor oxides or phase-changes need to be considered using CGS, implying changes in the microstructure just by cold-working and plastic deformation at the impact. With the low shrinkage and high strain induced on the impact leading to compressive stresses, the CGS-process gives the opportunity to apply higher thicknesses.

At the time CGS is the only process able to handle Ti6-4 without oxidation or nitration by chemical interaction with the process gas, due to the use of Helium as process gas without any electric heating or fuel gas needed. On the contrary side Helium as well as the equipment for CGS are more expensive than HVAF-spraying using unlimited compressed air and a cheap combustible to propel the powder and also being completely self-contained without the requirement for peripheral equipment such as independent cooling or oxygen tanks, also reducing the need for masking.

Both high-kinetic processes are limited in the choice of the substrate material: soft and friable substrates will be eroded by the processes. Hard and brittle materials cannot be sprayed by CGS in their pure form and need to be applied as composites with a ductile matrix-phase.

Taking all the facts into consideration HVAF-spraying proves as the cheaper, easier and better way to apply IN718 by thermal spraying, the CGS-process on the other hand being the state of the art to handle oxidation and temperature sensitive materials.

Acknowledgments

References

[1] Cold Spray Technoloy, Edited by Anatolii Papyrin; A. Papyrin, V. Kosarev, S. Klinkov; Elsevier, 2007

[2] Handbook of thermal spray technology, J.R. Davis; ASM International, 2004

[3] Activated Combustion HVAF Coatings for Protection against Wear and High Temperature Corrosion, *A. Verstak, V. Baranovski*, *UniqueCoat Technologies, Ashland, Virginia USA*

[4] Titan und Titanlegierungen, M. Peters & C. Leyens (Hrsg.), Wiley-VCH, 2002

[5] AMS 5596

[6] AMS 4911

[7] Volvo Aero Corporation Procedure V.AC:O-915382 000 (04): Provskiva (Cutting-Procedure)

[8] ASTM E562-08: Standard test method for determining volume fraction by systematic manual point count

[9] ASTM C633-01: Standard test method for adhesion or cohesion strength of thermal spray coating

[10] Volvo Aero Corporation Procedure V.AC:O-915387 000: Provberedning för Hårdhetstestning (Hot/Cold-Mounting-Procedure)

[11] Volvo Aero Corporation Procedure PST-338C: Rockwell Hardness Testing

[12] ASTM E18-08b: Standard test methods for Rockwell hardness of metallic materials

[13] Volvo Aero Corporation Procedure PST-337: Vickers Hardness Testing

[14] ASTM E384-10: Standard test method for microindentation hardness of materials

[15] Volvo Aero Corporation Procedure PST-347: VAC standard for surface roughness measurement

[16] Technical Report "Measurement of the Young`s-modulus of coated substrates"

[17] A Study of the Adhesion Strength of Plasma Sprayed Coatings; M. Fouzi Bahbou

[18] Grit Blasting as Surface Preparation before Plasma Spraying; Jan Wigren, Thermal Spray Technology, New Ideas and Processes, D.L. Houck, Oct. 24-27 1988, Cincinatti, OH, ASM Int. 1988, p. 99-104

[19] F. Kroupa, Nonlinear Behavior in Compression and Tension of Thermally Spayed Coatings, J. Therm. Spray Technol., 2007, 10(1), p.84-95

[20] Werkstoffwissenschaft, Worch, Schatt, Wiley-VCH

[21] Cathodic Deoxygenation of the Alpha Case on Titanium and Alloys in Molten Calcium Chloride, George Zheng Chen, Derek J. Fray, Tom W. Farthing

Table of Figures: